Linear nonequilibrium thermodynamics describes the dynamics of an autocatalytic system

Sonia Cortassa,*‡ Miguel A. Aon,* and Hans V. Westerhoff*‡
*E.C. Slater Institute for Biochemical Research, University of Amsterdam, NL-1018 TV Amsterdam; and ‡Netherlands Cancer Institute, H5, Division of Molecular Biology, NL-1066 CX Amsterdam, The Netherlands

ABSTRACT A model simulating oscillations in glycolysis was formulated in terms of nonequilibrium thermodynamics. In the kinetic rate equations every metabolite concentration was replaced with an exponential function of its chemical potential. This led to nonlinear relations between rates and chemical potentials. Each chemical potential was then expanded around its steady-state value as a Taylor series. The linear (first order) term of the Taylor series sufficed to simulate the dynamic behavior of the system, including the damped and even sustained oscillations at low substrate input or high free-energy load.

The glycolytic system is autocatalytic in that the number of ATP molecules produced in the second half of the pathway exceeds the number consumed in the first half. Because oscillations were obtained only in the presence of that autocatalytic feed-back loop we conclude that this type of kinetic nonlinearity was sufficient to account for the oscillatory behavior.

The matrix of phenomenological coefficients of the system is nonsymmetric. Our results indicate that it is the symmetry property and not the linearity of the flow-force relations in the near equilibrium domain that precludes oscillations. Given autocatalytic properties, a system exhibiting linear flow-force relations and being outside the near equilibrium domain may show bifurcations, leading to self-organized behavior.

INTRODUCTION

Self-organized phenomena, designated as dissipative structures (1), constitute one of the most challenging dynamic behaviors exhibited by metabolic networks. Stationary states may be spatially homogeneous and temporally monotonous (asymptotic) or spatially and/or temporally (self-)organized. Living organisms are spatio-temporally coherent. In part this coherence arises autonomously, by means of self-organization, which explains the interest in dissipative structures. Some general principles of organization of biological systems have been unravelled by nonequilibrium thermodynamics (1). One of these principles asserts the impossibility of self-organized spatio-temporal structures, such as autonomous oscillations and bistability, in the near equilibrium domain (1).

In spite of the importance of self-organization, biological applications of nonequilibrium thermodynamics (NET), have been limited to asymptotically stable steady states (2, 3), probably because NET used to be associated with near equilibrium systems. Recent extensions of NET, however, have transcended the near equilibrium region. The so-called Mosaic (M)NET has thereby been focusing on regions away from equilibrium with linear relations between "flows" (reaction rates and diffusion rates) and "forces" (free-energy differences) (4). More recently, a study of free-energy harvesting by an enzyme from an external oscillating field, introduced nonlinear flow-force relations to NET (5).

The question addressed in this work is whether this extended NET (MNET) is able to describe, at least qualitatively, self-organization. To answer this question, a model of glycolytic free-energy metabolism, with an autocatalytic feed back loop and an ATPase activity (6), has been formulated in terms of Mosaic Nonequilibrium Thermodynamics (4, 7, 8). Oscillatory behavior could be simulated with linear flow-force relations provided a positive autocatalytic feed back was present. The resulting matrix of phenomenological coefficients of the flow-force relation is highly asymmetric. This leads to the conclusion that the lack of symmetry of the flow-force relations rather than the absence of linearity is a necessary condition for self-organization to occur.

Address correspondence to Sonia Cortassa Instituto Superior de Investigaciones Biologicas (INSIBIOCONICET), Departamento Bioquimica de la Nutricion, Chacabuco 461, 4000-Tucuman, Argentina.

RESULTS

Rather than analyzing an abstract general scheme with little bearing on actual metabolism, the glycolytic pathway, which has been shown to exhibit oscillations under certain conditions (see reference 9 for a review), was considered. To obtain the simplest model still consistent with the oscillatory dynamic behavior, the starting point was a five-step kinetic model of glycolysis (6) which was simplified to a four-step model that still exhibited

0006-3495/91/10/794/10 $2.00

realistic oscillations (Fig. 1). The free variables in the glycolytic model were: [Glc], [FdP], and [ATP]. [ATP] and [ADP] were held interdependent through a conservation relation for adenine nucleotides: [ATP] + [ADP] = C_A, C_A being a constant. Except for a hyperbolic dependence of nonglycolytic ATP consumption on ATP, all rates were taken to be insensitive to product concentrations and first order in the concentrations of all their substrates.

In the expressions for the fluxes, each metabolite concentration in the classical, kinetic, rate equations was substituted for by the exponential function of its chemical potential with respect to a reference state (Eq. 8). These exponential functions were expanded around the steady state as a Taylor series and from the resulting nonlinear relations between rates and chemical potentials, only the zeroth and first order (linear) terms were taken into account.

DYNAMICS

To simulate the dynamic behavior of this linear nonequilibrium thermodynamic system, the time dependence of the free variables were written as the sum of the linear flow-force relations (Eqs. 16–18). The resulting system of differential equations (see Appendix Eqs. 16–18 after application of Eqs. 10–12 and 21) was integrated numerically using the SCoP package from the National Biomedical Simulation Resource (Duke University Medical Center, Durham, NC). The Adams subroutine was used with an integration step of 0.01 s.

At relatively high values of V_{in} and low loads (i.e., small values of k_P) the system exhibited a virtually monotonous evolution toward the steady state (Fig. 2 *a*) from various initial conditions. As V_{in} was decreased, damped oscillations appeared (Fig. 2 *b*). At high load (high k_P) sustained oscillations were observed in all metabolite concentrations (Fig. 2 *c*). This suggested the presence of a Hopf bifurcation point in the parameter space of the model (10, 11), as could be confirmed by stability analysis of the linearized system (see below).

The question arises as to which properties of the present system were required for it to exhibit self-organization. Nicolis and Prigogine (1) have pointed out that kinetic nonlinearity is one of the mechanisms that

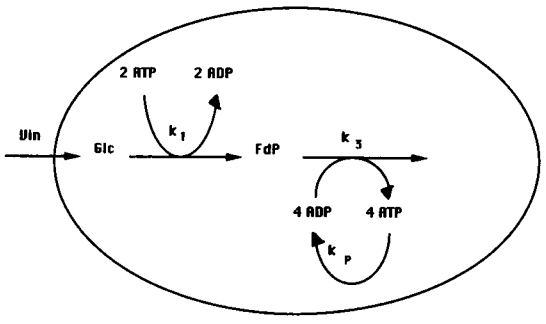

FIGURE 1 Schematic illustration of the glycolytic model. The four steps included in the model corresponded to (*a*) an influx of glucose, Glc, at a constant rate, (*b*) the conversion of a molecule of glucose to a molecule of the intermediate FdP under concomitant dephosphorylation of two molecules of ATP, (*c*) the disappearance of one molecule of FdP coupled to the phosphorylation of four molecules of ADP, and (*d*) a reaction hydrolysing ATP.

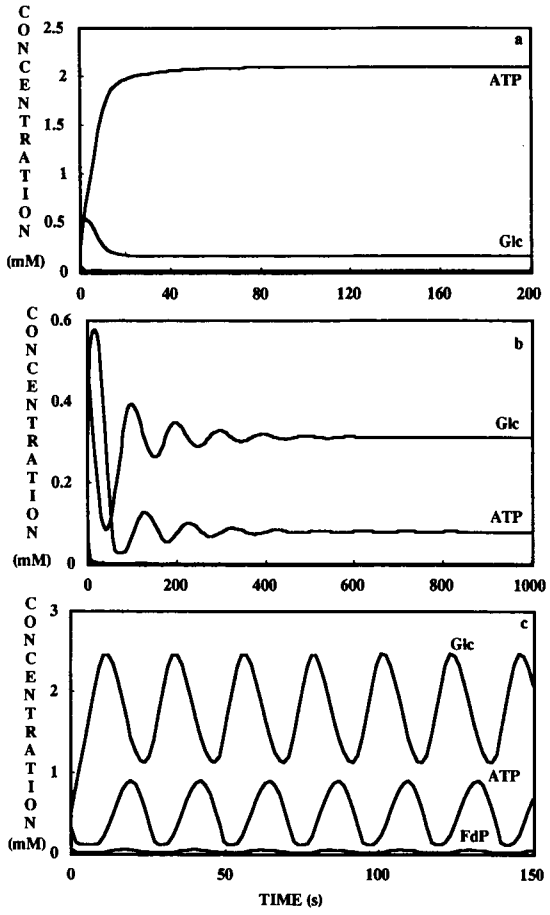

FIGURE 2 Temporal evolution of metabolite concentrations at various V_{in}. Eqs. 16–18, in combination with Eqs. 10–12 were integrated numerically for the following parameter values; $C_A = P_t = 10$ mM; $K_M = 2$ mM; (*a*) $V_{in} = 0.1$ mM s^{-1}; $k_P = 0.3905$ mM s^{-1}; $k_1 = 0.3$ mM^{-1} s^{-1}; $k_3 = 0.1$ mM^{-2} s^{-1}; (*b*) $V_{in} = 0.0075$ mM s^{-1}; $k_P = 0.3905$ mM s^{-1}; $k_1 = 0.3$ mM^{-1} s^{-1}; $k_3 = 0.1$ mM^{-2} s^{-1}; (*c*) $V_{in} = 0.2$ mM s^{-1}; $k_P = 2.5$ mM s^{-1}; $k_1 = 0.3$ mM^{-1} s^{-1}; $k_3 = 0.1$ mM^{-2} s^{-1}. The reference concentrations were taken equal to the steady-state values as obtained from Eq. 21 (in *c* this steady state was unstable). (*a*) $[Glc]_r = 0.159$ mM, $[ATP]_r = 2.0997$ mM, $[FdP]_r = 0.01266$ mM; (*b*) $[Glc]_r = 0.313$ mM, $[ATP]_r = 0.0799$ mM, $[FdP]_r = 0.000756$ mM; (*c*) $[Glc]_r = 1.75$ mM, $[ATP]_r = 0.3809$ mM, $[FdP]_r = 0.0208$ mM.

can be responsible for self-organization. The system used in the calculations presents an autocatalytic structure, in that the number of ATP molecules produced in the second step (k_3) exceeds the number consumed in the first step (k_1) (Fig. 1) (6). The question whether this positive feed back was required for the appearance of oscillations was addressed as follows. The feed back was eliminated in either of two ways: (*a*) by considering the first reaction (J_1) independent of [ATP], by setting $\gamma = 0$ in Eq. 13; (*b*) by equating the number of molecules of ATP consumed in the first step to the number produced in the second step (i.e., setting $n_1 = n_2 = 4$ in Eq. 17). In the latter case the load reaction characterized by k_P had to be eliminated. In both cases, oscillatory behavior could no longer be obtained (see Stability Analysis). This suggested that the positive feed back loop through [ATP] was required for the appearance of self-organized behavior in this system.

STABILITY ANALYSIS

The system given by Eqs. 16–18 was written as linear relations between the rate of change of a metabolite concentration and its chemical potential (Eq. 22). This system of equations was then reformulated as differential equations with the chemical potentials as variables (Eq. 28; see Appendix B). The characteristic equation of the Jacobian of Eq. 28 was solved analytically with a cubic equation algorithm. The three solutions were analyzed as functions of each of the kinetic parameters. The three solutions of the characteristic equation are the eigenvalues (1, 10) of the linear flow-force system given by Eqs. 16–18, or the linearized system represented by Eq. 28 and indicate the stability properties of these systems as well as the stability of the kinetic system (Eqs. 4–6) (6) from which the thermodynamic formulation has been derived. Fig. 3 indicates the parameter values for which (locally; close to the reference state) monotonous asymptotically stable behavior (*grey region*), damped oscillations (*diagonally hatched region*), or unstable spiralling (*vertically hatched region*) are expected. The thick line separating diagonally and vertically hatched regions corresponds to the Hopf bifurcation points, characterized by a pair of conjugate imaginary eigenvalues (10, 11). In the vertically hatched region where the eigenvalues of the Jacobian matrix are complex with positive real parts, indicating that the linear-thermodynamic system was unstable close to the reference state, the system did evolve toward stable limit cycles, corresponding to those shown in Fig. 4, *c–f* for the two dots in Fig. 3 *A*.

The latter evolution to a stable trajectory reflects that

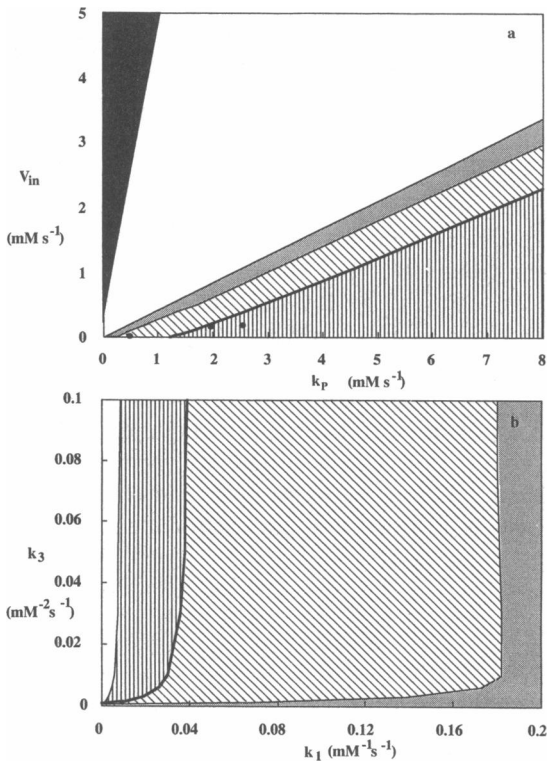

FIGURE 3 Bifurcation behavior of the glycolytic system for different sets of parameters. The analysis of the stability of the system as a function of the parameters was performed after transformation of variables from concentrations to chemical potentials and linearization of the corresponding differential equations (Appendix B). The eigenvalues of the corresponding Jacobian (Eq. 33, see Appendix B) were used as the stability criteria. The different shadings indicate distinct qualitative behavior as reflected by different kind of eigenvalues. In the black region, the reference concentrations calculated from Eq. 21 would take negative values; therefore this zone lacks physical meaning. The vertically hatched region corresponds to sets of parameters for which the system exhibited complex eigenvalues with positive real parts (the third eigenvalue was always real and negative); the reference state was unstable, i.e., states infinitesimally close to it evolve away from it in a spiralling fashion. In the parameter region depicted by diagonal hatches the system had two complex eigenvalues with negative real parts. Points around the reference state here spiralled back to it. The heavy line in between the two hatched areas indicate the Hopf bifurcation points; here two eigenvalues were purely imaginary conjugates. In the shaded region, all eigenvalues were real and negative, giving rise to nonoscillatory relaxation to the reference state. In the white region, all eigenvalues were real and were positive; states slightly deviating from the reference state develop monotonously away from it. In *a*, k_1 and k_3 were kept at 0.3 mM^{-1} s^{-1} and 0.1 mM^{-2} s^{-1}, respectively; in *b*, $V_{in} = 0.3$ mM s^{-1}; $k_P = 1.0$ mM s^{-1}. The values of the constants, C_A, P_i, and K_M, were as in Fig. 2.

stability analysis of the system linearized around the steady state, is not able to predict the stability properties of the entire phase space for that parametric domain (10). Only for linear systems with completely linear

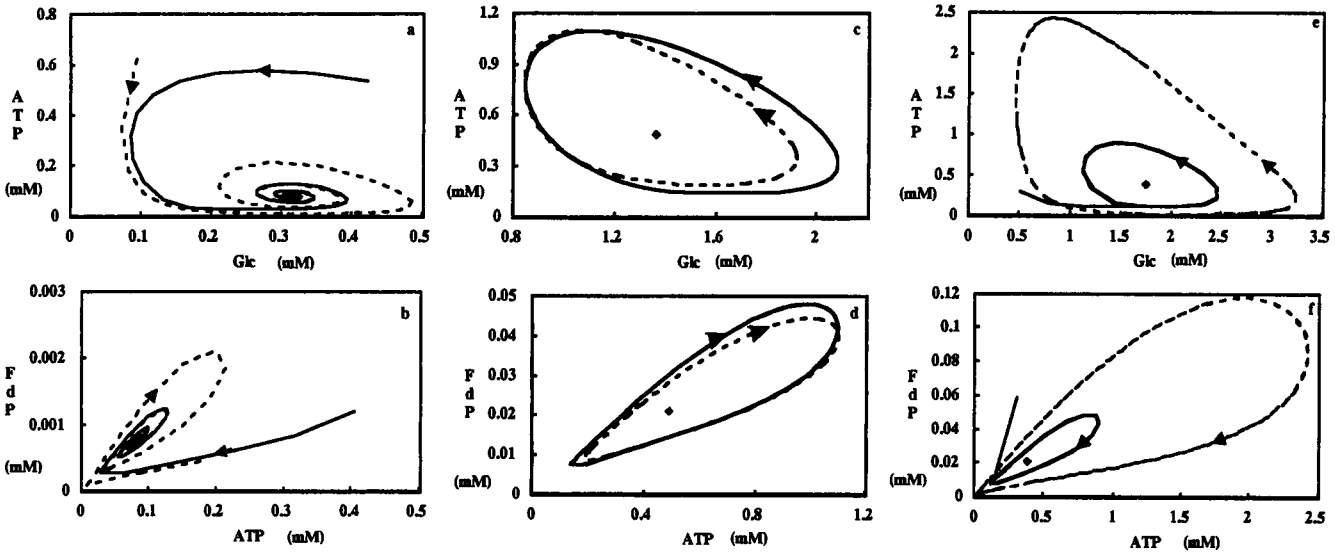

FIGURE 4 Phase plane analysis for the parameter sets corresponding to the three points indicated dots in Fig. 3. The plots represent the trajectories of the state variables for (a, b) $k_P = 0.3905$ mM s^{-1}; $k_1 = 0.3$ mM^{-1} s^{-1}; $k_3 = 0.1$ mM^{-2} s^{-1}, and $V_{in} = 0.0075$ mM s^{-1}; (c, d) $k_P = 2.033$ mM s^{-1}; $k_1 = 0.3$ mM^{-1} s^{-1}; $k_3 = 0.1$ mM^{-2} s^{-1}, and $V_{in} = 0.2$ mM s^{-1}; and (e, f) $k_P = 2.5$ mM s^{-1}; $k_1 = 0.3$ mM^{-1} s^{-1}; $k_3 = 0.1$ mM^{-2} s^{-1}, and $V_{in} = 0.2$ mM s^{-1}. In panels c–f the diamonds indicate the reference concentration that corresponds to the unstable steady state solution. The dashed lines represent the behavior of the kinetic model from which the linear thermodynamic model has been derived. The values of the constants, C_A, P_t, and K_M, were as in Fig. 2.

differential equations a single stability analysis is able to predict the dynamics in any parametric domain in the whole phase plane. The differential equations for the NET model presented here are nonlinear because of the autocatalytic feed back loop and the occurrence of both concentrations and their logarithms in Eq. 22.

Also the two nonautocatalytic systems described in the section DYNAMICS, *a* and *b*, were subjected to stability analysis. When the characteristic equations of the Jacobian of the corresponding linearized systems of both nonautocatalytic models were solved numerically for a broad parametric range ($V_{in} = 0.0001$–100 mM s^{-1}, $k_1 = 0.0001$–20 mM^{-1} s^{-1}, $k_3 = 0.0001$–20 mM^{-2} s^{-1}, and $k_P = 0.0001$–100 mM s^{-1}, the latter only for the nonautocatalytic system where γ in Eq. 13 is zero) not a single region with complex eigenvalues could be found.

Parameter space diagrams like that of Fig. 5 were obtained for the system that had no dependence of the first glycolytic step on [ATP] (model *a* in Dynamics). Only a region of unstable steady states was found by varying either V_{in} or k_P but no changes in the diagram were observed upon changes in the values of either k_1 or k_3. The system that did not contain a load and whose stoichiometric coefficients were equal for both glycolytic steps showed only real negative eigenvalues, i.e., just asymptotically stable steady states. This confirmed the earlier suggestion that the autocatalytic feed back

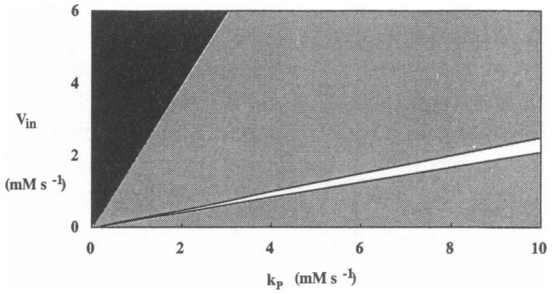

FIGURE 5 Bifurcation behavior of a nonautocatalytic version of the glycolytic system. The system analyzed in this diagram was as the one in Appendix A, and in Fig. 3 except that J_1 was taken to be [ATP] independent ($\gamma = 0$ in Eq. 13). The Jacobian of this system was derived as in the autocatalytic system (Eq. 33, Appendix B). Similar diagrams were obtained for various combinations of k_1 and k_3 in the following ranges: $k_1 = 0.0001$–20 mM^{-1} s^{-1}, $k_3 = 0.0001$–20 mM^{-2} s^{-1}. The dynamics of the system were deduced from the eigenvalues, obtained by solving the characteristic equation of the Jacobian. The shadings have the same meaning as in Fig. 3. In the black region the reference concentrations would take negative values; therefore this zone lacks physical meaning. In the shaded region, all eigenvalues were real and negative, giving rise to nonoscillatory relaxation to the reference state. The nonshaded region corresponds to unstable monotonous regimes (real positive eigenvalues).

through ATP was the nonlinearity involved in the appearance of oscillations.

COMPARING KINETIC AND NONEQUILIBRIUM THERMODYNAMIC DESCRIPTIONS

In this paper, the starting point was a kinetic model which was translated into a nonlinear NET model and then linearized. As a consequence of the latter linearization, the linear NET model used here is only an approximation of the original kinetic model, whenever other states than the reference state are considered. This has no implications for the local stability properties around (stable or unstable) steady states (Appendix B, Eq. 33 and its discussion).

It does have implications, however, for the dynamics of evolution toward stable steady states. In Figs. 4 *a* and *b*, we demonstrate this: the full line is the evolution for the NET model, whereas the dashed line indicates the evolution for the kinetic model from which the NET model was derived as a first order approximation. Not unexpectedly the two descriptions become more similar as the ratios of the concentrations to the corresponding concentrations in the reference state become much less than the base of natural logarithms, *e*. And, as also shown in Fig. 4, *a* and *b*, the kinetic and NET descriptions will end up in the same stable steady state.

Around unstable steady states, the fact that the linear NET model is only an approximation of the kinetic model, has more conspicuous implications for the simulated dynamic behavior. When the system evolves to a limit cycle, the limit cycle described by the linear NET description may differ from that described by the corresponding kinetic description. However, for bifurcation parameter values close to the Hopf bifurcation point the (linear) thermodynamic description was still quantitatively similar to the kinetic description (Fig. 4, *c* and *d*, *dashed lines*). In the parametric region of sustained oscillations, the amplitude of a limit cycle increased as the bifurcation parameter was taken further away from the Hopf bifurcation point, allowing the chemical potentials of metabolites to deviate strongly from the steady-state values. In those cases the MNET model was not able to predict quantitatively the time dependence of metabolite concentrations. The linear thermodynamic description could, however, predict the type of dynamic behavior in the entire parametric space of the kinetic model. Therefore the linear approximation has primarily a qualitative value when applied at unstable steady states.

DISCUSSION

The main finding of the present work is the occurrence of self-organized dynamic behavior, namely autonomous oscillations, for a realistic metabolic system with linear flow force relations.

For a further evaluation of the results it is relevant to discuss the meaning of "force" and "linearity" as used in the context of this work.

MEANINGS OF "FORCE" AND "LINEARITY"

It may be argued that the chemical potential of a substrate is not a force in the thermodynamic sense because the force of a given reaction is the free-energy difference between substrates and products of that reaction. However, as the reaction scheme is irreversible, the flux through a given step will be "blind" with respect to the activity of the product (12, 13) as the water flow from a high waterfall is independent of the potential energy difference but only depends on the amount of water at the top. This hydrodynamical analogy suggests that also a chemical potential may act as a force for irreversible reactions. Indeed, the thermodynamic description in terms of the chemical potentials of their substrates alone of Michaelian reaction flows insensitive to product concentrations is accepted practice in NET (12, 13).

Likewise, it is important to distinguish the various meanings of the word linearity as currently used in the literature. Any dependence of a rate law on the concentration of a compound to a power different from 1 produces nonlinear kinetics. Any positive or negative feed-back or feed-forward loop transforms the kinetic structure of a system to a nonlinear one.

With respect to linearity in the sense of NET, the relations between the flows and the thermodynamic forces may be expanded into a Taylor series around any reference point. If only a small range of variation in the forces is considered, the second and highest order terms of the Taylor series may be neglected and the first order term may be considered as a good approximation to describe the flux. This type of NET linearity, which will be called approximative linearity, is strictly dependent on variations in the forces being much smaller than RT. Translation of kinetic rate equations into NET rate equations (8, 12, 13) has revealed that there also exist values of the forces around which there is the so-called extended linearity. There, the second term of the Taylor series need not be neglected because it is zero by itself.

LINEARITIES AND NONLINEARITIES IN THE GLYCOLYTIC MODEL

Except for the nonglycolytic ATP-consuming reaction the kinetic equations of the individual steps that served as the basis for the flow force relations were kinetically linear with respect to each metabolite. As J_1 and J_3 are bisubstrate reactions, the kinetic laws that described them were bilinear. Our thermodynamic formulation of the kinetic model (Eqs. 10–12 and 13–15) was "linear" in the usual nonequilibrium thermodynamic sense, i.e., the individual fluxes were linear functions of the logarithms of the substrate concentrations. However, the corresponding differential equations (Eq. 22) were nonlinear in the sense that the rate of change of the concentration of a metabolite depended linearly on the logarithm of its own concentration as well as on the logarithm of other metabolite concentrations. In addition, there was an autocatalytic feed-back loop arising from the fact that the number of ATP molecules produced in the second reaction (k_3) exceeds the number consumed in the first step (k_1). This autocatalytic feature of glycolysis provides for an added kinetic nonlinearity. In the present model the autocatalysis and not the mathematical nonlinearity arising from the relation between the rate of change of the concentration of a metabolite and the logarithms of its own or other metabolite concentrations was indispensable for the appearance of self-organized behavior (see Stability analysis) (14). Of course, other models of glycolysis lead to self-organized behavior on the basis of the kinetic nonlinearity of a single enzyme, namely phosphofructokinase (9, 10).

That in the present calculations, the nonlinearity arising from the autocatalytic structure of the system was indispensable for self-organized behavior was confirmed in two ways: (*a*) by abolishing the dependence of the first glycolytic step on ATP concentration and (*b*) by equating the stoichiometric coefficients of the ATP-producing and ATP-consuming reactions. In either case, when the Jacobian of the transformed variable system was solved, no region with complex eigenvalues could be found in the parametric space (Fig. 5).

The autocatalytic type of kinetic nonlinearity discussed above, has implications for the sign of the phenomenological coefficients (e.g., such that the dependence of J_1 on μ_{ATP} is positive even though ATP is a pathway product) and not necessarily for the linearity of the relationship between the flow and the force. Indeed, the type of autocatalysis described in this work was shown to coexist with linear flow-force correlations (6). However, in reference 6 the oscillations appeared in regions of nonlinear correlations between fluxes and forces.

In the limit cycles appearing farther from the Hopf bifurcation points the forces became large compared with RT. Thus, the quantitative aspects of the dynamics differed from those described with a kinetic model (Fig. 4). However, the qualitative thermodynamic description of the dynamics of this system is identical to that obtained with the kinetic model.

LINEARITY AND SYMMETRY PROPERTIES OUTSIDE THE NEAR EQUILIBRIUM DOMAIN

Most NET (2, 15, 16) treatments were limited to the near-equilibrium region, defined as the region where all the forces deviated much less than RT from equilibrium. Because of this limitation imposed on the variations in the forces, the flow-force relations could be approximated by linear (proportional) ones. In addition, in the near equilibrium domain the phenomenological cross-coefficients are equal, a property known as Onsager symmetry (15, 16). This symmetry property cannot be guaranteed outside the near equilibrium domain (1, 3, 4).

Most biological systems operate farther from equilibrium than RT. In quite a few such systems, linear flow-force relations have been observed (3, 8, 12, 13, 17–20). Although nonlinear free-energy converters can function quite efficiently (21), the fact that under certain conditions, linear and symmetrical free-energy converters may be up to 10^6 or 10^9 times more efficient than their nonlinear counterparts, has led to the conjecture that, through evolution, biological free-energy transducing systems may have acquired some kind of sophisticated feed-back regulation, which maintains this linearity and symmetry (22). It has also been proposed that some far-from-equilibrium forces may poise metabolic reactions to the near equilibrium domain (20). That in the corresponding experimental system (20), the symmetry property of that domain is also fulfilled, has not been demonstrated.

The question whether linearity in the sense of NET would preclude the occurrence of oscillations in a system with an autocatalytic kinetic structure, was investigated. By expanding the dependencies of the fluxes on the forces linearly, the flow-force relations had been forced to be linear. The linear flow force relations used were characteristic of thermodynamic linearity away from the near equilibrium domain. Oscillations were indeed described by this "linear" MNET model.

The conclusion that linearity per se is not in conflict with self-organized behavior does not contradict the demonstration (1) that self-organization cannot be observed close to equilibrium: it is the symmetry property

of the near-equilibrium domain (13, 14) and not the linearity often attached to it, that precludes self-organized behavior (1). Indeed, the flow-force relations used in the calculations (Eqs. 10–12) were not symmetric.

It has been proven that self-organization (1, 23, 24) can only occur further than RT away from equilibrium (1, 23). Kinetic schemes involving only linear kinetics and not containing feed back or feed forward do not exhibit bifurcations (1, 25), precluding self-organized behavior to arise. On the other hand, kinetic nonlinearities may lead to self-organization.

An important implication of the present work is that the linear flow-force relations found in an autocatalytic biological system, away from equilibrium, do not necessarily prevent such systems from exhibiting self-organized behavior. Indeed, linear relations between reaction rates and thermodynamic forces will generally not lead to a Jacobian matrix with only real eigenvalues. The dynamic behavior of the system, i.e., whether the system will undergo a bifurcation (as a parameter is varied) and change from, e.g., a monotonous asymptotic behavior to oscillatory steady states, is not determined by thermodynamic linearity but by the particular values of the kinetic parameters. Therefore, it is not the linearity of the flow-force relations but the kinetic structure, contained implicitly in the phenomenological coefficients (L's) of the MNET equations, which has the information about the dynamics of a given system.

APPENDIX A

In the present calculations, glycolysis is depicted as resulting from individual fluxes corresponding to different steps of the pathway related through conservation equations (6)

$$V_1 = k_1[Glc][ATP] \tag{1}$$

$$V_3 = k_3[FdP](C_A - [ATP])P_i \tag{2}$$

$$V_P = k_P \frac{[ATP]}{K_M + [ATP]}. \tag{3}$$

k_1 and k_3 are the kinetic rate constants of the first (upper) and second (lower) glycolytic steps, respectively; k_P is a lumped constant for nonglycolytic ATP-consuming processes (load) and P_i is the phosphate concentration assumed to be constant. K_M is the Michaelis constant of the ATPase.

The system is described by the following set of differential equations, including a conservation relationship for adenine nucleotides:

$$\frac{d[Glc]}{dt} = Vin - V_1 \tag{4}$$

$$\frac{d[ATP]}{dt} = -2V_1 + 4V_3 - V_P \tag{5}$$

$$\frac{d[FdP]}{dt} = V_1 - V_3 \tag{6}$$

$$C_A = [ATP] + [ADP]. \tag{7}$$

To obtain the nonequilibrium thermodynamic description, first, kinetic rate equations (6) were written with linear dependencies on the substrate concentrations. An exception was made from the ATPase reaction which was assumed to depend hyperbolically on the concentration of ATP. To make the transition to the nonlinear thermodynamic model, the concentrations were then expressed into the corresponding chemical potentials (8, 12, 13), using:

$$\frac{[M]}{[M]_r} = \exp\left(\frac{\mu_M - \mu_M^r}{RT}\right). \tag{8}$$

The linear nonequilibrium thermodynamic description was obtained by expanding each exponential function of a chemical potential as its Taylor series around an arbitrary reference state:

$$\exp\left(\frac{\mu_M - \mu_M^r}{RT}\right) = 1 + \frac{\mu_M - \mu_M^r}{RT} + \frac{1}{2}\frac{(\mu_M - \mu_M^r)^2}{(RT)^2} + \frac{1}{6}\frac{(\mu_M - \mu_M^r)^3}{(RT)^3} + \cdots \tag{9}$$

and neglecting all but the first two terms. As in the MNET formalism (4, 7), the flux through each of the steps, J_i, was expressed as a function of the, offset (4, 8), chemical potentials of the substrates of that particular step multiplied by a coefficient L containing implicitly the kinetic information concerning rate constants and the reference concentrations. This led to the following expressions for the fluxes:

$$J_1 = k_1[ATP]_r[Glc]_r\left(1 + ln\frac{[ATP]}{[ATP]_r} + ln\frac{[Glc]}{[Glc]_r}\right) \tag{10}$$

$$J_3 = k_3P_i(C_A - [ATP]_r)[FdP]_r \cdot \left(1 + ln\frac{(C_A - [ATP])}{(C_a - [ATP]_r)} + ln\frac{[FdP]}{[FdP]_r}\right) \tag{11}$$

$$J_P = k_P\frac{[ATP]_r}{K_M + [ATP]_r}\left(1 + \frac{K_M}{K_M + [ATP]_r}ln\frac{[ATP]}{[ATP]_r}\right). \tag{12}$$

The preceding formulation of the fluxes is analogous to the implicit form of NET in terms of linear flow-force relations:

$$J_1 = L_1(\mu_{Glc} + \gamma\mu_{ATP} + C_1) \tag{13}$$

$$J_3 = L_3(\mu_{FdP} + \mu_{ADP} + C_3) \tag{14}$$

$$J_P = L_P(\mu_{ATP} + C_P). \tag{15}$$

With $\gamma = 1$.

Interpreting the chemical potential as driving force (cf. Discussion) Eqs. 10–12 and 13–15 correspond to the linear flow-force relations for the present system. According to Fig. 1, the fluxes imply the following rates of changes of the metabolite concentrations:

$$\frac{d[Glc]}{dt} = Vin - J_1 \tag{16}$$

$$\frac{d[ATP]}{dt} = -n_1J_1 + n_2J_3 - J_P; \quad n_1 = 2, n_2 = 4 \tag{17}$$

$$\frac{d[FdP]}{dt} = J_1 - J_3. \quad (18)$$

V_{in} represents the input rate of substrate, namely glucose. The dependence on [ATP] of the flux J_3 (Eq. 11) was calculated through the following conservation relation for the adenine nucleotide pool:

$$C_A = [ATP] + [ADP]. \quad (19)$$

In this stoichiometric model the reference concentrations are parameters which affect the quantitative and qualitative behavior of the system. The reference state was chosen as the steady state defined by:

$$\frac{d[Glc]}{dt} = \frac{d[ATP]}{dt} = \frac{d[FdP]}{dt} = 0. \quad (20)$$

Eqs. 10–12 plus 20 reveal the concentrations of ATP, Glc, and FdP of the reference state:

$$[ATP]_r = \frac{2K_M Vin}{k_P - 2Vin}; \quad [Glc]_r = \frac{k_P - 2Vin}{2K_M k_1};$$

$$[FdP] = \frac{Vin}{k_3 P_t \left(C_A - \frac{2K_M Vin}{k_P - 2Vin}\right)}. \quad (21)$$

In our calculations the steady state will be taken as the reference state. This choice does not preclude that the system under some circumstances will exhibit sustained oscillations. Stability analysis (not shown) has revealed that, under such conditions, the states defined by expression (21) correspond to unstable steady states.

APPENDIX B

The stability analysis was performed by linearization of the equations around the steady state and determination of the system's eigenvalues through solution of the characteristic equation of Jacobian matrix. A transformation of variable was necessary since the differential equations (Eqs. 16–18 plus 10–12) expressed changes in concentrations (e.g., $d[Glc]/dt$) as functions of the chemical potentials of the metabolites involved (e.g., $ln[Glc]/[Glc]_r$). The procedure for the variable transformation was as follows:

$$\begin{bmatrix} \dot{[Glc]} \\ \dot{[ATP]} \\ \dot{[FdP]} \end{bmatrix} = \mathbf{M} \cdot \begin{bmatrix} ln\frac{[Glc]}{[Glc]_r} \\ ln\frac{[ATP]}{[ATP]_r} \\ ln\frac{[FdP]}{[FdP]_r} \end{bmatrix} + c, \quad (22)$$

where the matrix **M** stands for the Jacobian of the system depicted in Eqs. 10–12 and 16–18 and **c** is a vector of constants. Superscript dot refers to the time derivative of the variable. In Eq. 11 J_3 was dependent on [ATP] through the conservation relation (Eq. 19). To derive the corresponding element of the matrix **M** the expression of the logarithm containing the [ATP] was subjected to Taylor series expansion in terms of the ln[ATP]. The derivative of the first-order term of this series with respect to the logarithm of [ATP] related to the reference concentration was used in evaluating the corresponding elements of M.

To obtain differential equations in terms of logarithms of concentrations, we transformed the state variables [Glc], [ATP], and [FdP] to σ, α, and β defined by:

$$\sigma = ln\frac{[Glc]}{[Glc]_r} \quad \alpha = ln\frac{[ATP]}{[ATP]_r} \quad \beta = ln\frac{[FdP]}{[FdP]_r} \quad (23)$$

$$\frac{dln[Glc]}{dt} = \dot{\sigma} \quad \frac{dln[ATP]}{dt} = \dot{\alpha} \quad \frac{dln[FdP]}{dt} = \dot{\beta}. \quad (24)$$

In terms of the new variables, the system (22) can be written as:

$$\begin{bmatrix} e^{\sigma} & 0 & 0 \\ 0 & e^{\alpha} & 0 \\ 0 & 0 & e^{\beta} \end{bmatrix} \cdot \begin{bmatrix} [Glc]_r & 0 & 0 \\ 0 & [ATP]_r & 0 \\ 0 & 0 & [FdP]_r \end{bmatrix} \cdot \begin{bmatrix} \dot{\sigma} \\ \dot{\alpha} \\ \dot{\beta} \end{bmatrix} = \mathbf{M} \cdot \begin{bmatrix} \sigma \\ \alpha \\ \beta \end{bmatrix} + \mathbf{c}. \quad (25)$$

These equations were linearized by expanding the inverse of the matrix on the left hand side and neglecting second and higher order terms:

$$\begin{bmatrix} e^{-\sigma} & 0 & 0 \\ 0 & e^{-\alpha} & 0 \\ 0 & 0 & e^{-\beta} \end{bmatrix} \cong \begin{bmatrix} 1 & 0 & 0 \\ 0 & 1 & 0 \\ 0 & 0 & 1 \end{bmatrix} - \begin{bmatrix} \sigma & 0 & 0 \\ 0 & \alpha & 0 \\ 0 & 0 & \beta \end{bmatrix}. \quad (26)$$

Multiplying Eqs. 25 and 26 side by side results in:

$$\begin{bmatrix} \dot{\sigma} \\ \dot{\alpha} \\ \dot{\beta} \end{bmatrix} = S_r^{-1}\mathbf{M} \begin{bmatrix} \sigma \\ \alpha \\ \beta \end{bmatrix} - S_r^{-1} \begin{bmatrix} \sigma & 0 & 0 \\ 0 & \alpha & 0 \\ 0 & 0 & \beta \end{bmatrix} \mathbf{M} \begin{bmatrix} \sigma \\ \alpha \\ \beta \end{bmatrix} + Sr^{-1}\,\mathbf{c} - S_r^{-1} \begin{bmatrix} \sigma & 0 & 0 \\ 0 & \alpha & 0 \\ 0 & 0 & \beta \end{bmatrix} \mathbf{c}. \quad (27)$$

Neglecting the second term in the right hand side of Eq. 27 we may rewrite this equation as:

$$\begin{bmatrix} \dot{\sigma} \\ \dot{\alpha} \\ \dot{\beta} \end{bmatrix} \cong \mathbf{N} \cdot \begin{bmatrix} \sigma \\ \alpha \\ \beta \end{bmatrix} + \mathbf{S}_r^{-1} \cdot \mathbf{c}, \quad (28)$$

where:

$$\mathbf{S}_r^{-1} = \begin{bmatrix} [Glc]_r & 0 & 0 \\ 0 & [ATP]_r & 0 \\ 0 & 0 & [FdP]_r \end{bmatrix}^{-1} \quad (29)$$

if **C** the diagonal matrix having the elements of vector **c** on its main diagonal and zeros elsewhere:

$$\begin{bmatrix} \sigma & 0 & 0 \\ 0 & \alpha & 0 \\ 0 & 0 & \beta \end{bmatrix} \mathbf{c} = \mathbf{C} \begin{bmatrix} \sigma \\ \alpha \\ \beta \end{bmatrix}. \quad (30)$$

Unlike the Jacobian of the kinetic system, the Jacobian of the nonequilibrium thermodynamics transformed system, N, explicitly contains information deriving from the constants c:

$$\mathbf{N} = \mathbf{S}_r^{-1} \cdot \mathbf{M} - \mathbf{S}_r^{-1} \cdot \mathbf{C}. \tag{31}$$

Yet, for any specific case, the constant c are related to the kinetic parameters (4; cf. Eqs. 10–12 to Eqs. 13–15). Indeed if N_k is the Jacobian of the system of kinetic differential equations (Eqs. 4–6), from which the system of NET differential equations was derived as first order approximation, then:

$$\mathbf{N} = \mathbf{S}_r^{-1} \cdot \mathbf{N}_k \cdot \mathbf{S}_r. \tag{32}$$

In terms of the kinetic parameters, N reads:

$$\begin{bmatrix} -\dfrac{Vin}{[Glc]_r} & -k_1[ATP]_r & 0 \\ -2k_1[Glc]_r & 4k_3P_t[FdP]_r\dfrac{-C_A}{[ATP]_r} + k_P\dfrac{[ATP]_r}{(K_M+[ATP]_r)^2} & 4k_3\dfrac{P_t[FdP]_r(C_A-[ATP]_r)}{[ATP]_r} \\ k_1\dfrac{[ATP]_r[Glc]_r}{[FdP]_r} & k_1\dfrac{[ATP]_r[Glc]_r}{[FdP]_r} - k_3P_t(C_A-[ATP]_r)\dfrac{-[ATP]_r}{(C_A-[ATP]_r)} & -k_1\dfrac{[ATP]_r[Glc]_r}{[FdP]_r} \end{bmatrix} \tag{33}$$

The characteristic cubic equation for this Jacobian matrix,

$$\det\left\{\mathbf{N} - \lambda \cdot \begin{bmatrix} 1 & 0 & 0 \\ 0 & 1 & 0 \\ 0 & 0 & 1 \end{bmatrix}\right\} = 0 \tag{34}$$

was solved analytically. The characteristics (i.e., complex vs. real, negative vs. positive real parts) of the three roots, corresponding to the three eigenvalues of N were used as criterium for the stability properties of the system at given parameter values.

We thank Dr. K van Dam for stimulating discussions and Dr. D Kahn for helpful criticism. We thank H. Stoffers for writing some of the software used and the U.S. National Biomedical Simulation Resource for providing us with the SCoP program.

Dr. Cortassa and Aon are thankful to the European Economic Community for financial support. In part this work was supported by the Netherlands Organization for Scientific Research (NWO).

Received for publication 2 January 1991 and in final form 19 March 1991.

REFERENCES

1. Nicolis, G., and I. Prigogine. 1977. Self-organization in nonequilibrium systems. John Wiley, New York.
2. Katchalsky, A., and P. F. Curran. 1965. Non Equilibrium Thermodynamics in Biophysics. Harvard University Press, Cambridge, MA.
3. Caplan, S. R., and A. Essig. 1983. Bioenergetics and linear nonequilibrium thermodynamics. The steady state. Harvard University Press, Cambridge, MA.
4. Westerhoff, H. V., and K. van Dam. 1987. Thermodynamics and control of biological free-energy transduction. Elsevier, Amsterdam.
5. Astumian, R. D., P. B., Chock, T. Y. Tsong, and H. V. Westerhoff. 1989. Effects of oscillations and energy-driven fluctuations on the dynamics of enzyme catalysis and free-energy transduction. *Physical Reviews A.* 39:6416–6435.
6. Cortassa, S., M. A. Aon, and D. Thomas. 1990. Thermodynamic and kinetic studies in a stoichiometric model of energetic metabolism under starvation conditions. *FEMS (Fed. Eur. Microbiol. Soc.) Microbiol. Lett.* 66:249–256.
7. Westerhoff, H. V., J. S. Lolkema, R. Otto, and K. Hellingwerf. 1982. Thermodynamics of growth. Non-equilibrium thermodynamics of bacterial growth. The phenomenological and the mosaic approach. *Biochim. Biophys. Acta.* 683:181–220.
8. Van der Meer, R., H. V. Westerhoff, and K. van Dam. 1980. Linear relation between rate and thermodynamic force in enzyme catalyzed reactions. *Biochim. Biophys. Acta.* 591:488–493.
9. Goldbeter, A., and S. R. Caplan. 1976. *Annu. Rev. Biophys. Bioeng.* 5:449–476.
10. Segel, L. A. 1980. Models in Molecular and Cellular Biology. Cambridge University Press, Cambridge, UK.
11. Hopf, E. 1942. Abzweigung einer periodischen Lösung von einer stationären Lösung eines Differentialsystems. *Ber. Math. Kl. Schs Phys. Akad. Wiss. Leipzig.* 94:3–22.
12. Rottenberg, H. 1973. The thermodynamic description of enzyme catalyzed reactions. The linear relation between the reaction rate and the affinity. *Biophys. J.* 13:503–511.
13. Rothschild, K. J., S. A. Ellias, A. Essig, and H. E. Stanley. 1980. Nonequilibrium linear behavior of biological systems. Existence of enzyme mediated multidimensional inflection points. *Biophys. J.* 30:209–230.
14. Westerhoff, H. V., M. A. Aon, K. van Dam, S. Cortassa, D. Kahn, and M. van Workum. 1990. Dynamical and hierarchical coupling. *Biochim. Biophys. Acta.* 1018:142–146.
15. Onsager, L. 1931. Reciprocal relations in irreversible processes I. *Physiol. Rev.* 37:405–426.
16. Onsager, L. 1931. Reciprocal relations in irreversible processes II. *Physiol. Rev.* 38:2265–2279.
17. Van Dam, K., H. V. Westerhoff, K. Krab, R. Van der Meer, and J. C. Arents. 1980. Relationship between chemiosmotic flows and thermodynamic forces in oxidative phosphorylation. *Biochim. Biophys. Acta.* 591:240–250.
18. Wanders, R. J. A., and H. V. Westerhoff. 1988. Sigmoidal relation between mitochondrial respiration and log $([ATP]/[ATP])_{out}$ under conditions of extramitochondrial ATP utilization. Implications for the control and thermodynamics of oxidative phosphorylation. *Biochemistry.* 27:7832–7840.
19. Stucki, J. W. 1980. The optimal efficiency and the economic degrees of coupling of oxidative phosphorylation. *Eur. J. Biochem.* 109:269–283.
20. Berry, M. N., R. B. Gregory, A. R. Grivell, D. C. Henly, J. W. Phillips, P. G. Wallace, and G. R. Welch. 1987. Linear relationships between mitochondrial forces and cytoplasmic flows argue

for the organized energy-coupled nature of cellular metabolism. *FEBS (Fed. Eur. Biochem. Soc.) Lett.* 224:201–207.

21. Juretic, D., and H. V. Westerhoff. 1987. Variation in efficiency with free-energy dissipation in models of biological energy transduction. *Biophys. Chem.* 28:21–34.
22. Stucki, J. W., M. Compiani, and S. R. Caplan. 1983. Efficiency of energy conversion in model biological pumps. Optimization by linear nonequilibrium thermodynamic relations. *Biophys. Chem.* 18:101–109.
23. Glansdorff, P., and I. Prigogine. 1971. Thermodynamic theory of structure, stability and fluctuations. Wiley, London.
24. Haken, H. 1977. Synergetics. Springer, Berlin.
25. Hyver, C. 1972. Impossibility of existence of undamped oscillations in linear chemical systems. *J. Theor. Biol.* 36:133–138.